actuators

MDPI

Article

Actuator-Oriented Analytical Efficiency Modelling of Planetary Gear Transmissions Under Reduction and Multiplication Modes

Haoyuan Pan [1,2,†], Mikhail E. Lustenkov [2,*,†], Andrei Korneev [2], Gennady Lenevsky [2] and Yitong Niu [2,3,*]

[1] School of Technology and Business Management, Bazhong Vocational and Technical College, Bazhong 636000, China
[2] School of Electrical Engineering, Belarusian-Russian University, 212030 Mogilev, Belarus
[3] School of Industrial Technology, Universiti Sains Malaysia, Minden 11800, Penang, Malaysia
* Correspondence: lustenkov@yandex.by (M.E.L.); ytniu@student.usm.my (Y.N.)
† These authors contributed equally to this work.

Abstract

Planetary gear trains (PGTs) are core transmission units in high-ratio mechanical systems, including vehicle drivetrains, industrial reducers, robotic joints, and servo mechanisms, where transmission efficiency affects power demand, thermal loading, actuator sizing, housing reaction, and self-locking risk. This study develops a unified analytical framework for estimating the efficiency of involute PGTs used in actuator-oriented systems. The formulation covers common 2k–h and k–h–v layouts, single- and double-rim satellites, reduction and multiplication modes, and different assignments of driving, driven, and stationary members. Starting from power balance, Willis' relation, and torque equilibrium, compact closed-form expressions are derived by representing mesh losses through the efficiency of the reverted mechanism. The resulting baselines quantify the effects of transmission ratio, mesh efficiency, operating mode, self-locking boundary, and housing-reaction torque. The results show that multiplication mode becomes more sensitive to loss amplification as mesh efficiency decreases, especially in k–h–v configurations approaching the self-locking boundary. Double-rim 2k–h configurations also exhibit branch-dependent efficiency and housing-torque behavior. For representative duty-cycle calculations, increasing gear-train efficiency from 0.85 to 0.92 reduces motion energy by approximately 7–8%. The framework provides a lightweight tool for early-stage actuator-transmission screening before detailed modelling, dynamic simulation, or prototype testing.

Keywords: planetary gear train; transmission efficiency; analytical modelling; reverted mechanism; reduction and multiplication modes; self-locking

Academic Editor: Dong Jiang

Received: 20 June 2026
Revised: 9 July 2026
Accepted: 12 July 2026
Published: 14 July 2026

1. Introduction

Planetary gear trains (PGTs) are widely used in high-ratio mechanical transmissions, including vehicle powertrains, industrial reducers, robotic gearboxes, and precision servo mechanisms, because they provide compact coaxial power flow, torque multiplication, and load sharing within limited installation space [1–5]. In these systems, transmission efficiency directly affects power demand, heat generation, thermal margins, and motor or actuator sizing, particularly under variable load and speed conditions [6,7]. Experimental studies on planetary gear sets have further shown that losses are strongly affected by operating speed, transmitted torque, oil temperature, lubrication conditions, and test configuration [8–10]. Similar concerns have been reported for industrial planetary reducers and high-speed planetary reducers, where power-loss estimation is needed during early drivetrain development before detailed thermal modelling or prototype testing is available [11,12]. Therefore, a compact analytical efficiency baseline is useful for screening planetary-gear layouts and identifying operating regions where loss amplification, self-locking, or unfavorable torque reactions may become important.

During preliminary transmission design, detailed loss measurements, thermal-network simulations, and tribological models are often unavailable because material selection, lubricant specification, bearing arrangement, and housing geometry may not yet be fixed [13–15]. Analytical efficiency models therefore remain useful for comparing candidate planetary layouts at prescribed transmission ratios before prototype testing or high-fidelity simulation is undertaken [16,17]. Earlier studies have shown that planetary-gear efficiency can be derived from speed relations, torque balance, power-flow analysis, and equivalent mesh-loss assumptions, providing a practical basis for design-stage evaluation [18,19]. However, the usefulness of such models depends on whether the formulation remains consistent across operating modes, topological arrangements, and link assignments. This requirement becomes especially important for compound or multi-link planetary mechanisms, where attainable transmission-ratio ranges, internal power flow, recirculation, and efficiency ranges are strongly coupled to the selected constructive solution [20]. A compact formulation should therefore apply uniformly to common planetary topologies, remain valid in both reduction and multiplication modes, and avoid dependence on arbitrary choices of input, output, or stationary member.

Many analytical formulations evaluate planetary-gear efficiency by reducing the actual train to one or more reverted or equivalent mechanisms, in which local mesh losses are represented by equivalent mesh efficiencies and combined with speed and torque relations [21–23]. Although this strategy is compact, the available formula sets are not always directly transferable across operating modes, power-flow patterns, and link assignments. Pennestrì and Valentini reviewed different formulas for two-degree-of-freedom epicyclic gear trains and showed that several approaches are equivalent only under their stated assumptions, while some require redundant input data [24]. Later analyses of two-degree-of-freedom planetary gear units further showed that Radzimovsky-type relations have restricted validity and that power-flow direction, virtual or potential power, and branch power circulation must be treated explicitly [25,26]. Consequently, changes in sign convention, carrier-power treatment, reverted-mechanism ratio, or mesh-efficiency assignment can lead to different efficiency expressions and different interpretations of self-locking or loss amplification. These issues motivate a formulation that keeps the functional roles of the driving, driven, and stationary members explicit while producing mode-consistent efficiency expressions for the 2k–h and k–h–v layouts considered here.

Analytical efficiency research on planetary transmissions has also expanded beyond canonical three-link mechanisms. Four-, five-, and six-link planetary gear trains have been analyzed to determine attainable transmission-ratio and efficiency ranges, showing that constructive layout strongly affects both kinematic feasibility and efficiency behavior [27]. Power-flow and loss models have also been developed for two-degree-of-freedom and differential epicyclic gear trains, where internal power circulation and branch-dependent torque paths complicate efficiency prediction [24,26]. In parallel, compact high-ratio variants, including one-tooth-difference planetary reducers and cycloidal-pin transmissions, have been investigated because they offer large reduction ratios within limited installation space but involve different contact conditions, loss pathways, and output-transfer mechanisms [28–30]. These studies demonstrate the breadth of planetary-transmission design, but they also indicate the need for a compact formulation focused on common involute 2k–h and k–h–v layouts, where reduction and multiplication modes can be compared under a consistent efficiency framework.

Against this background, this paper presents a unified analytical framework for efficiency estimation of involute planetary gear transmissions used in actuator-oriented mechanical systems. The novelty of the work does not lie in treating each planetary-gear family in isolation, but in consolidating common 2k–h and k–h–v layouts, single- and double-rim satellite arrangements, reduction and multiplication modes, and different assignments of driving, driven, and stationary members within a consistent closed-form formalism. Starting from power balance, Willis' relation, and torque equilibrium along the transmission axis, the proposed method represents mesh losses through the efficiency of the reverted mechanism and derives mode-consistent efficiency expressions across the considered layouts. This unified formulation makes it possible to compare transmission-ratio effects, mesh-efficiency sensitivity, self-locking boundaries, and housing-reaction torque behavior under the same sign convention and power-flow interpretation. By linking these quantities to actuator power demand and duty-cycle energy use, the framework provides a lightweight basis for early-stage planetary-transmission screening, actuator pre-sizing, and mechanical-system assessment before detailed tribological modelling, dynamic simulation, or prototype testing is undertaken.

2. Methods

2.1. Analytical Formulation of Planetary Gear Efficiency

A planetary reducer or multiplier is treated here as a one-degree-of-freedom mechanism composed of three principal links: the driving link (in), the driven link (out), and the stationary link (stop). In line with established efficiency formulations for epicyclic and planetary gear trains, the transmission efficiency is defined from the ratio of output power to input power [16,18]:

$$\eta_{\text{in-out}}^{\text{stop}} = -\frac{P_{out}}{P_{\text{in}}} = -\frac{T_{\text{out}} \cdot \omega_{\text{out}}}{T_{\text{in}} \cdot \omega_{\text{in}}} \quad (1)$$

where P_{in} and P_{out} are the input and output powers, T_{in} and T_{out} are the input and output torques, and ω_{in} and ω_{out} are the corresponding angular velocities. Equation (1) follows directly from the power balance relation $P_{\text{in}} + P_{\text{out}} + P_{\text{stop}} = 0$, or equivalently $T_{\text{in}} \cdot \omega_{\text{in}} \cdot \eta_{\text{in-out}}^{\text{stop}} + T_{\text{out}} \cdot \omega_{\text{out}} + T_{\text{stop}} \cdot \omega_{\text{stop}} = 0$. For $\omega_{stop} = 0$, Equation (1) is obtained. This definition expresses efficiency in terms of power rather than accumulated work, which is more convenient for analytical derivation because work increases indefinitely with angular displacement. Under constant shaft speeds, the same expression can also be interpreted in an average sense. In the present study, losses associated with bearings and lubricant agitation are not modelled explicitly; instead, the analysis focuses on the mesh-related contribution to transmission efficiency [17].

To evaluate the efficiency of a planetary gear train, several sign conventions are introduced. The driving shaft is assumed to rotate in the positive direction, defined as counterclockwise with respect to the transmission axis directed from the driving shaft toward the driven shaft. A positive torque acts on the driving shaft, meaning that the torque and angular velocity vectors have the same direction. The rotation direction of the driven link is determined after the transmission ratio has been established. For the driven shaft, the torque vector is opposite to the angular velocity vector because it represents the resisting load torque.

With these conventions, the power associated with the driving link is positive, whereas that associated with the driven link is negative. The negative sign in Equation (1) therefore ensures that efficiency remains a positive scalar quantity between zero and one. Values approaching zero indicate very poor transmission performance, whereas zero or negative values inferred from the force balance correspond to self-locking conditions.

The efficiency analysis is based on the reverted mechanism, that is, the equivalent mechanism with a stationary carrier. Its efficiency, denoted by η_0, is assumed to be known and is written as the product of the efficiencies of the sequential gear meshes in the reverted configuration, i.e., $\eta_0 = \eta_1 \cdot \eta_2 \cdot \ldots \cdot \eta_n$, where $\eta_1, \eta_2, \ldots, \eta_n$ are the efficiencies of the individual meshing pairs. This treatment aggregates local mesh losses into a single physically interpretable parameter and provides a compact basis for the subsequent derivations. Two additional relations are employed. The first is the vector equilibrium condition of the torques acting along the transmission axis:

$$\overrightarrow{T_{in}} + \overrightarrow{T_{out}} + \overrightarrow{T_{stop}} = 0 \tag{2}$$

The second is Willis' relation for the reverted mechanism:

$$\frac{\omega_{in} - \omega_h}{\omega_{out} - \omega_h} = i_0^h \tag{3}$$

where ω_h is the angular velocity of the carrier and i_0^h is the transmission ratio of the reverted mechanism.

The analytical procedure can be summarized as follows. First, the transmission ratio of the reverted mechanism, i_0^h, is determined from the gear tooth numbers while preserving the functional role of the driving member. In this construction, the stationary link of the analyzed transmission becomes the driven link of the reverted mechanism; if the carrier is the driving member in the analyzed configuration, the stationary element becomes the driver in the reverted mechanism. Second, Willis' relation is used to express the transmission ratio of the actual configuration in terms of i_0^h, from which the directions of the angular velocities and torques of the driven link are established. Third, the vector torque balance in Equation (2) is projected onto the transmission axis to obtain a scalar torque relation with signs assigned according to the adopted direction conventions. Fourth, Equation (1) is applied to the reverted mechanism to express the torque ratio between the driving and driven members as a function of i_0^h and η_0. Finally, this torque ratio is substituted back into Equation (1) for the analyzed planetary transmission to obtain the overall efficiency in terms of i_0^h and η_0.

This procedure is applied to the most common planetary configurations considered in this study, namely, the 2k–h arrangement with a single-rim satellite, the k–h–v arrangement with a single-rim satellite, and the 2k–h arrangement with a double-rim satellite, as illustrated in Figure 1.

2.2. Analytical Workflow and Operating-Point Assumptions

The analytical procedure used in this study is summarized in Figure 2. The purpose of the workflow is to provide a closed-form screening route for planetary gear transmissions used in actuator-oriented mechanical systems. For each candidate configuration, the required inputs are the planetary topology, gear tooth numbers, functional member assignment, operating mode, and reverted-mechanism efficiency. The topology defines whether the analyzed system corresponds to a 2k–h or k–h–v layout and whether single- or double-rim satellites are used. The functional member assignment specifies the driving, driven, and stationary members, whereas the operating mode distinguishes reduction from multiplication.

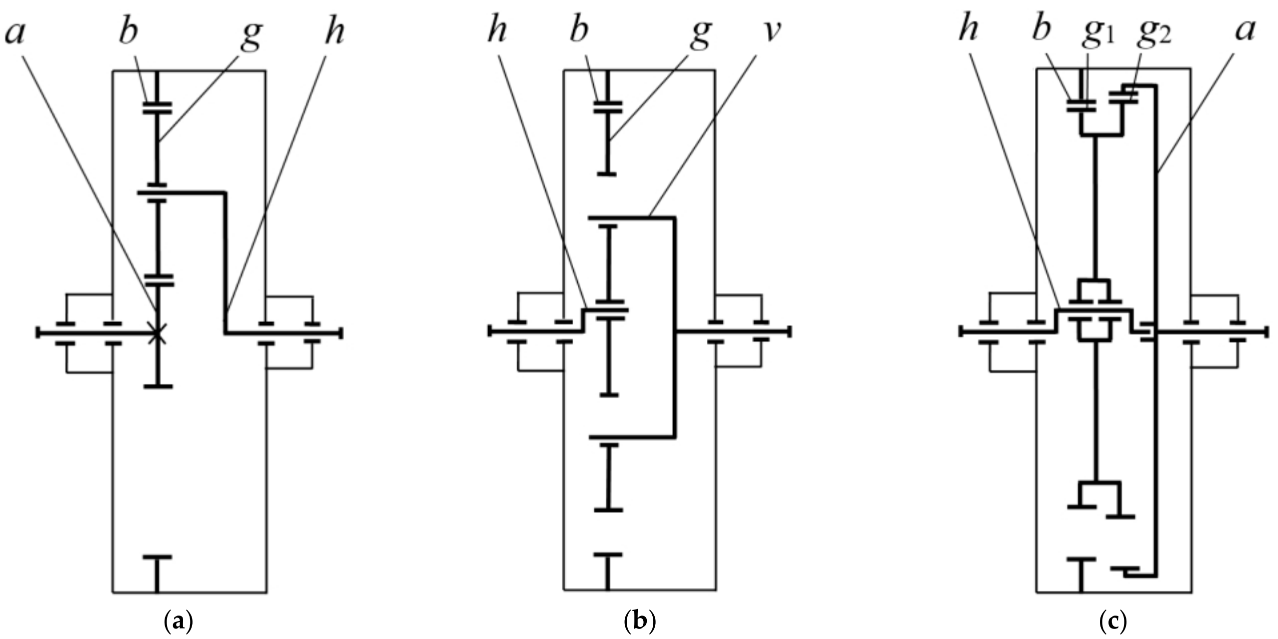

Figure 1. Schematics of planetary gear systems: (**a**) 2k-h with a single-rim satellite; (**b**) k-h-v with a single-rim satellite; (**c**) 2k-h with a double-rim satellite.

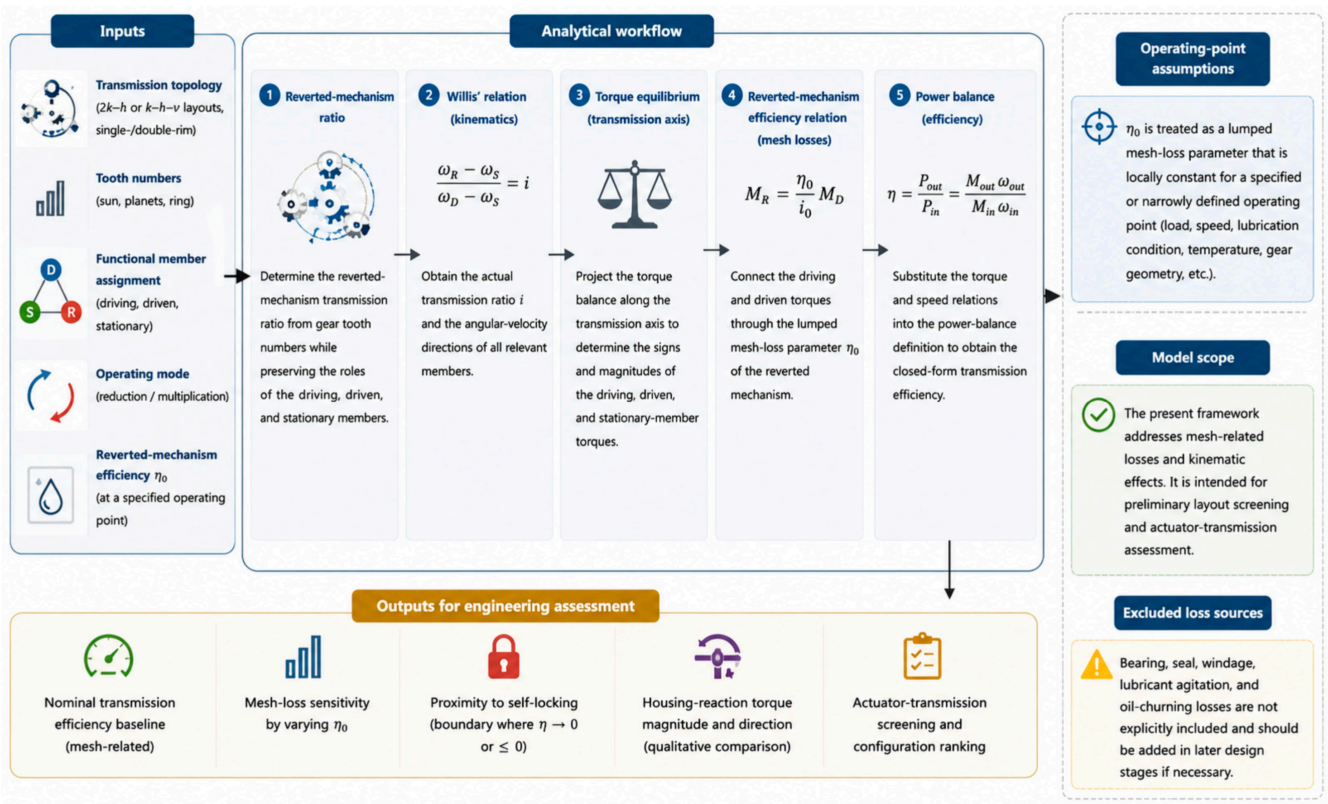

Figure 2. Analytical workflow for actuator-oriented planetary-transmission efficiency screening.

Starting from these inputs, the reverted-mechanism transmission ratio is first determined from the gear tooth numbers while preserving the functional roles of the members. Willis' relation is then applied to obtain the actual transmission ratio and the angular-velocity directions of the relevant links. The torque-equilibrium relation is subsequently projected along the transmission axis to determine the signs and relative magnitudes of the driving, driven, and stationary-member torque components. The efficiency relation of the reverted mechanism is used to connect the torque ratio with the lumped mesh-loss parameter, η_0. Finally, the resulting torque and speed relations are substituted into the power-balance definition of transmission efficiency to obtain the closed-form efficiency expression for the selected configuration.

The outputs of the workflow are engineering baselines for preliminary actuator-transmission assessment. These include the nominal mesh-related efficiency baseline, the sensitivity of transmission efficiency to changes in η_0, the tendency of a configuration to approach self-locking, the qualitative housing-reaction torque condition, and the suitability of a configuration for actuator-transmission screening. These outputs are intended to support early-stage layout comparison before detailed tooth-contact analysis, thermal modelling, lubricant-loss modelling, dynamic simulation, or prototype testing is performed.

Within this workflow, the reverted-mechanism efficiency, η_0, should be understood as a local operating-point parameter rather than as a universal constant of the gear train. In practical transmissions, mesh efficiency may vary with transmitted load, rotational speed, lubrication regime, oil temperature, surface roughness, tooth geometry, profile modification, and assembly condition. The present formulation therefore treats η_0 as locally constant only for a specified or narrowly defined operating condition. When the operating condition changes substantially, η_0 should be updated or expressed as a function of the relevant operating and design variables. Varying η_0 over a prescribed range is therefore used here as a sensitivity analysis of mesh-loss deterioration rather than as a fixed-efficiency assumption over all duty conditions.

2.3. Self-Locking Criterion and Full-Loss Interpretation

The self-locking condition is evaluated within the same power-balance framework used for the efficiency derivation. For a transmission operating in the intended direction, useful power transfer requires positive output power after the internal mesh losses have been overcome. Therefore, the self-locking boundary is defined here as the limiting condition at which the useful output power tends to zero and the calculated transmission efficiency approaches zero. If the analytical expression gives zero or non-positive efficiency, the corresponding operating point is regarded as self-locking or physically infeasible for the intended power-flow direction. In practical terms, this means that the available driving power is no longer sufficient to overcome the internal losses and maintain motion of the driven member.

This criterion is especially important in multiplication mode. In this mode, power is transmitted through the reverse path of the planetary mechanism, and the effect of mesh losses can be amplified by the transmission-ratio structure. As the absolute value of the transmission ratio increases, a larger fraction of the input power is consumed internally. The calculated efficiency may therefore decrease rapidly and approach zero. Such behavior should not be interpreted only as low efficiency; rather, it indicates that the mechanism is approaching the self-locking boundary. Operating regions close to this boundary should be treated as self-locking-prone and should not be selected for reversible or speed-increasing actuator applications without further verification.

The efficiency obtained from the analytical expressions in this study should also be interpreted as a mesh-related baseline rather than as the total efficiency of a complete gearbox. The reverted-mechanism efficiency represents the effective loss level associated with gear meshing in the corresponding reverted mechanism. Bearing losses, seal losses, windage, lubricant agitation, and oil-churning losses are not explicitly included in the closed-form expressions. These losses may be small in low-speed or lightly lubricated preliminary comparisons, but they can become significant in high-speed planetary reducers, oil-bath transmissions, compact sealed actuator gearboxes, or heavily loaded bearing arrangements.

For a fully specified actuator gearbox, the total efficiency should therefore be evaluated by combining the present mesh-related baseline with additional loss contributions. Conceptually, the total efficiency may be viewed as the mesh-related efficiency corrected by bearing, seal, windage, churning, thermal, and other design-specific loss factors. The present model is thus intended to identify favorable kinematic layouts, sensitive transmission-ratio ranges, and self-locking-prone regions before detailed tribological modelling, thermal analysis, multibody simulation, or prototype testing is performed.

3. Results

3.1. Efficiency Characteristics of 2k–h Planetary Gear Trains with Single-Rim Satellites

As shown in Figure 1a, the 2k–h planetary gear train with a single-rim satellite consists of two central gears, a and b, and a carrier h. In the most common reduction configuration, gear a acts as the driving member, gear b is fixed, and the carrier h is the driven member. The corresponding directions of angular velocities and torques are illustrated in Figure 3a. For the reverted mechanism with a stationary carrier, the efficiencies of the external mesh between gear a and satellite g, η_{ag}, and of the internal mesh between satellite g and gear b, η_{gb}, are assumed to be known; hence, the efficiency of the reverted mechanism is $\eta_0 = \eta_{ag}\eta_{gb}$.

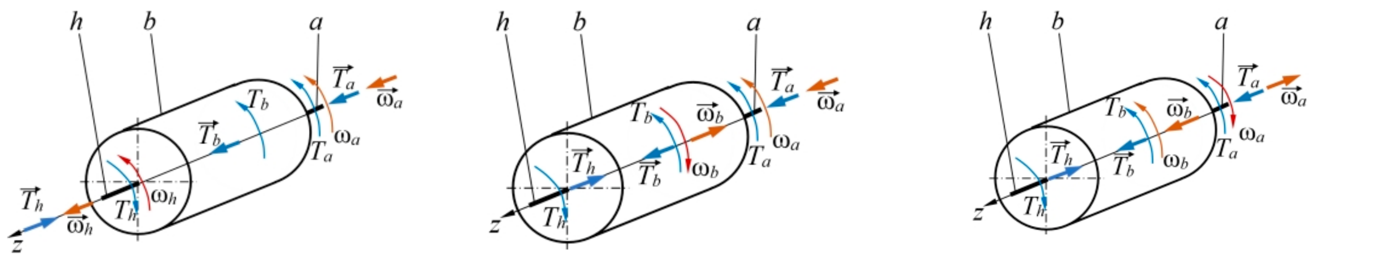

Figure 3. Directions of angular velocities and torques in the 2k–h planetary gear system with a single-rim satellite: (**a**) torque transmission $a \to h$; (**b**) reverted mechanism $a \to b$; (**c**) torque transmission $b \to h$.

In the reverted mechanism, gear a remains the driving member, whereas gear b becomes the driven member. The corresponding transmission ratio is as follows:

$$i_{ab}^{h} = \frac{\omega_a}{\omega_b} = -\frac{Z_g \cdot Z_b}{Z_a \cdot Z_g} = -\frac{Z_b}{Z_a} \tag{4}$$

As shown in Figure 3b, the carrier is stationary in the reverted configuration. From Equation (3), taking $\omega_b = 0$, one obtains the following:

$$\begin{gathered} \frac{\omega_a - \omega_h}{-\omega_h} = i_{ab}^{h} \\ -\frac{\omega_a}{\omega_h} + 1 = i_{ab}^{h} \\ i_{ab}^{h} = 1 - i_{ah}^{b} \end{gathered} \tag{5}$$

Substituting Equation (4) into Equation (5) gives

$$i_{ah}^{b} = 1 - i_{ab}^{h} = 1 + \frac{Z_b}{Z_a} \tag{6}$$

Since $i_{ab}^{h} \le -1$, the limiting value -1 is reached when $Z_a = Z_b$, which is possible in bevel-gear transmissions with $\Theta = \pi/2$ rad, as illustrated in Figure 4c. At $Z_a > Z_b$, a transmission scheme analogous to those shown in Figures 1a and 4a,b is obtained, in which the larger wheel becomes the driving wheel; this case is considered separately below. From Equation (5), it follows that $i_{ah}^{b} \geq 2$. Therefore, the absolute value of the resisting torque on the driven link exceeds that on the driving link, and the torque equilibrium along the transmission axis is written as follows:

$$\begin{aligned} T_a + T_b + T_h &= 0 \\ T_h &= -(T_a + T_b) \end{aligned} \tag{7}$$

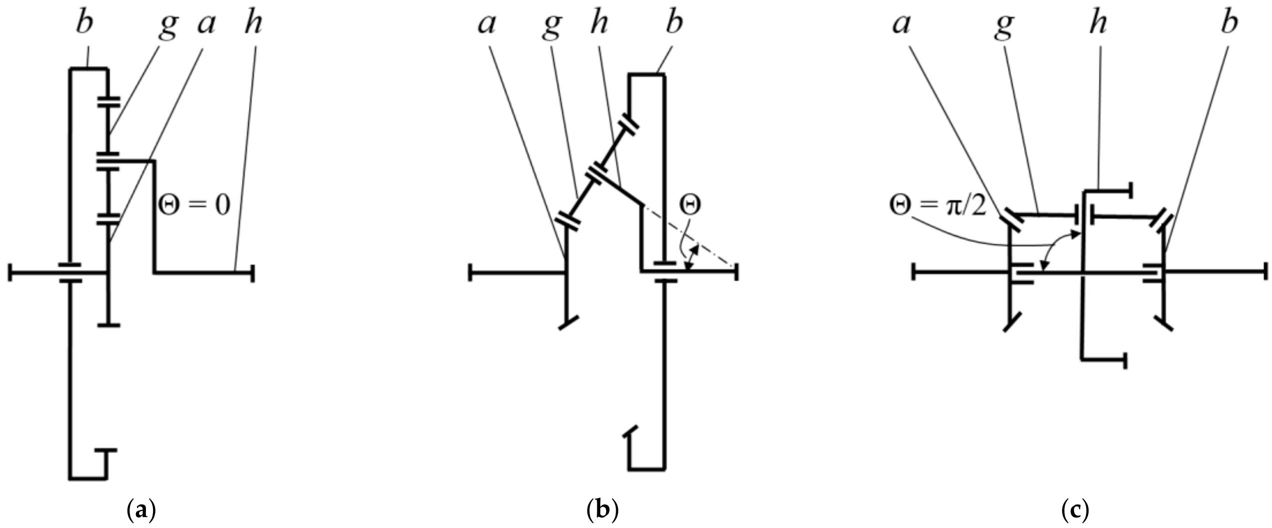

Figure 4. Planetary gear mechanisms with cylindrical (**a**) and bevel (**b**,**c**) gears.

Applying Equation (1) to the reverted mechanism yields the following:

$$\begin{aligned} &\eta_0 = -\tfrac{P_b}{P_a} = -\tfrac{T_b \cdot \omega_b}{T_a \cdot \omega_a} = -\tfrac{T_b}{T_a \cdot i_{ab}^{h}} \\ &-\eta_0 \cdot i_{ab}^{h} = \tfrac{T_b}{T_a} \end{aligned} \tag{8}$$

Substituting Equations (5), (7), and (8) into Equation (1), the transmission efficiency of the 2k–h mechanism with gear a as the driver and carrier h as the driven member is obtained as follows:

$$\eta_{ah}^{b} = -\frac{P_h}{P_a} = -\frac{T_h \cdot \omega_h}{T_a \cdot \omega_a} = -\frac{-(T_a + T_b)}{T_a} \cdot \frac{1}{i_{ah}^{b}} = \left(1 - \eta_0 \cdot i_{ab}^{h}\right) \cdot \frac{1}{i_{ah}^{b}} = \frac{1 - \eta_0 \cdot i_{ab}^{h}}{1 - i_{ab}^{h}} \tag{9}$$

As an example, consider a three-satellite planetary gear train with $Z_a = 21$ and $Z_b = 63$. If $\eta_{ag} = 0.97$ and $\eta_{gb} = 0.98$, then $\eta_0 = \eta_{ag}\eta_{gb} = 0.951$. The corresponding transmission ratios are $i_{ab}^{h} = -3$ and $i_{ah}^{b} = 4$, and Equation (9) gives $\eta_{ah}^{b} = 0.963$, which is slightly higher than the efficiency of the reverted mechanism.

When gear b is the driving member and carrier h is the driven member, the directions of angular velocities and torques for the reverted mechanism are shown in Figure 3c. By analogy with Equation (9), the efficiency of the mechanism is as follows:

$$\eta_{bh}^{a} = \frac{1 - \eta_0 \cdot i_{ba}^{h}}{1 - i_{ba}^{h}} \tag{10}$$

with the following corresponding transmission ratios:

$$\begin{aligned} &i_{ba}^{h} = -\tfrac{Z_a}{Z_b} \\ &i_{bh}^{a} = 1 - i_{ba}^{h} = 1 + \tfrac{Z_a}{Z_b} \end{aligned} \tag{11}$$

For the same numerical example, Equation (10) gives $\eta^{a}_{bh} = 0.988$. Thus, when the larger central wheel acts as the driving member and the carrier is the output, the transmission efficiency becomes higher. In general, Equations (9) and (10) can be written as follows:

$$\eta^{\text{stop}}_{in-h} = \frac{1 - \eta_0 \cdot i^h_{\text{in-stop}}}{1 - i^h_{in-stop}} = \frac{i^h_{\text{stop-in}} - \eta_0}{i^h_{\text{stop-in}} - 1} \tag{12}$$

where

$$\begin{aligned} i^h_{in-stop} &= -\tfrac{Z_{stop}}{Z_{in}} \\ i^h_{stop-in} &= \tfrac{1}{i^h_{in-stop}} = -\tfrac{Z_{in}}{Z_{stop}} \end{aligned} \tag{13}$$

Here, Z_{in} and Z_{stop} denote the numbers of teeth on the driving and stationary gears, respectively.

When the carrier is the driving member and gear a is the driven member, a multiplying transmission is obtained. In determining the transmission ratio of the reverted mechanism, the role of the driven link is retained for the driven link of the analyzed transmission, so that gear b becomes the driver in the reverted scheme: $i_{hba} = \frac{\omega_b}{\omega_a} = -\frac{Z_a}{Z_b}$.

From Willis' relation, the transmission ratio of the analyzed mechanism is $i_{bha} = i_{hba}/(i_{hba} - 1)$, which may be expressed through tooth numbers as $i_{bha} = Z_a/(Z_a + Z_b)$. Equation (8) is correspondingly transformed into $T_a/T_b = -i_{hba}\eta_0$. The efficiency of the multiplying transmission is then

$$\eta^b_{ha} = -\frac{P_a}{P_h} = -\frac{T_a \cdot \omega_a}{-(T_a + T_b) \cdot \omega_h} = \frac{1}{1 - \left(\frac{1}{i^h_{ba} \cdot \eta_0}\right) \cdot i^b_{ha}} = \frac{i^h_{ba} - 1}{\frac{1}{\eta_0} - 1} \tag{14}$$

The gear ratios of the reverted mechanisms with different driving links are inversely related. Expressing the efficiency through i^h_{ab} gives the following:

$$\eta^b_{ha} = \frac{1 - i^h_{ab}}{1 - \frac{i^h_{ab}}{\eta_0}} \tag{15}$$

and, in general form

$$\begin{aligned} \eta^{stop}_{h-out} &= \frac{1 - i^h_{out-stop}}{i^h_{out-stop}} \\ \eta_0 &= \frac{i^h_{stop-out} - 1}{i^h_{stop-out} - \frac{1}{\eta_0}} \end{aligned} \tag{16}$$

where

$$\begin{aligned} i^h_{out-stop} &= -\tfrac{Z_{stop}}{Z_{out}} \\ i^h_{stop-out} &= -\tfrac{Z_{out}}{Z_{stop}} \end{aligned} \tag{17}$$

Comparison of Equations (12) and (16) shows that the reduction and multiplication cases are not described by identical expressions, even though they belong to the same kinematic family. This distinction reflects the different torque-transfer characteristics of the two operating modes. Their behavior over the practically relevant transmission-ratio range is summarized in Figure 5.

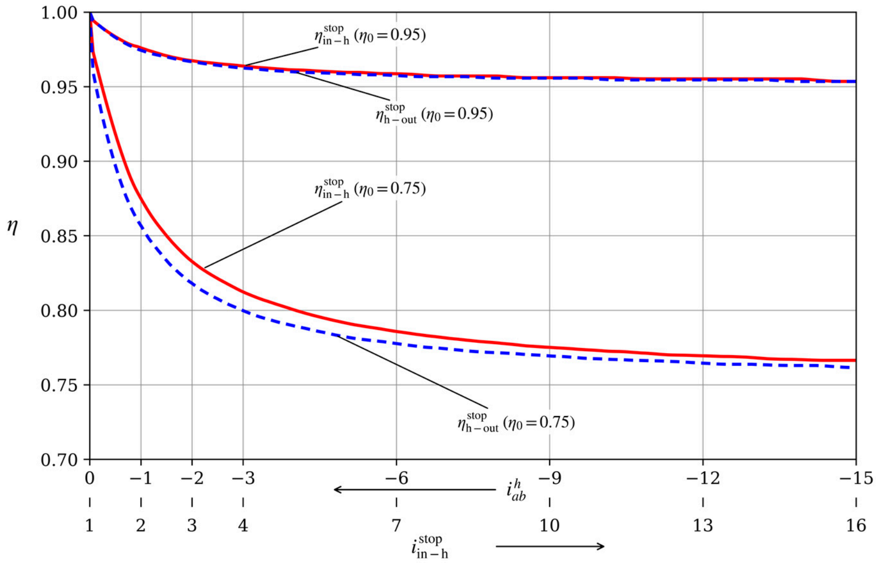

Figure 5. Efficiency baselines of 2k–h planetary gear trains with single-rim satellites as functions of transmission ratio and reverted-mechanism loss level.

As shown in Figure 5, when the meshing efficiencies are high, for example $\eta_{ag} = 0.97$, $\eta_{gb} = 0.98$, and $\eta_0 \approx 0.95$, the efficiency curves for reduction and multiplication modes are nearly identical, with differences only in the thousandths range. When the meshing efficiencies decrease, for example $\eta_{ag} = 0.86$, $\eta_{gb} = 0.87$, and $\eta_0 \approx 0.75$, the transmission efficiency decreases progressively as the absolute value of the transmission ratio increases. Under these less favorable meshing conditions, the decrease is more pronounced in multiplication mode than in reduction mode. This indicates that the multiplier regime is inherently more sensitive to loss amplification and therefore provides a more responsive operating region for detecting efficiency deterioration.

From an engineering-design perspective, the curves in Figure 5 can be interpreted as nominal efficiency baselines for the 2k–h single-rim configuration. Under a fixed transmission-ratio magnitude, the separation between reducer and multiplier curves indicates how strongly each operating mode penalizes reductions in mesh efficiency. The 2k–h single-rim arrangement therefore provides a useful reference for comparing reducer and multiplier operation and for identifying ratio ranges where the efficiency margin becomes more sensitive to mesh-loss deterioration.

3.2. Efficiency Characteristics of k–h–v Planetary Gear Trains with Single-Rim Satellites

For the k–h–v configuration with a single-rim satellite, the carrier h acts as the driving member and the satellite g acts as the driven member in reduction mode. In this case, the overall transmission efficiency is determined by the efficiency of the gear mesh together with that of the mechanism transmitting motion from the satellite to the output shaft. In the present derivation, only the gear-mesh-related contribution is considered explicitly, whereas losses associated with the output transfer mechanism depend on its specific structural realization, such as Hooke's-joint-based or crank-based arrangements, and are therefore excluded from the closed-form efficiency expression.

To derive the transmission efficiency, the reverted mechanism with a stationary carrier is analyzed while retaining the driven function of satellite g and assigning gear b as the driving member. The transmission ratio of the reverted mechanism is written as follows:

$$i^h_{bg} = \frac{\omega_b}{\omega_g} = \frac{Z_g}{Z_b} \tag{18}$$

From Equation (3), with $\omega_h = 0$, one obtains the relations for the analyzed transmission, which lead to the following:

$$\begin{gathered} \frac{-\omega_h}{\omega_g-\omega_h} = i^h_{bg} \\ i^b_{hg} = \frac{\omega_h}{\omega_g} = \frac{i^h_{bg}}{i^h_{bg}-1} = \frac{1}{1-i^h_{gb}} = \frac{Z_g}{Z_g-Z_b} \end{gathered} \tag{19}$$

Since $z_b > z_g$ (in cylindrical gears), the gear ratio of the considered transmission will be negative. The angular velocities of the carrier and the satellite will be in opposite directions, while the torques on the carrier and satellite will align. The efficiency of the inversion mechanism is as follows:

$$\begin{gathered} \eta_0 = -\frac{T_g \cdot \omega_g}{T_b \cdot \omega_b} = -\frac{T_g}{T_b \cdot i^h_{bg}} \\ \frac{T_b}{T_g} = -\frac{1}{i^h_{bg} \cdot \eta_0} \end{gathered} \tag{20}$$

Substituting the torque relation derived from Equation (20) together with Equation (19) into the general power-balance formulation yields the efficiency of the k–h–v transmission in reduction mode:

$$\eta^b_{hg} = -\frac{P_g}{P_h} = -\frac{T_g \cdot \omega_g}{(T_g + T_b) \cdot \omega_h} = \frac{i^h_{bg} - 1}{i^h_{bg} - \frac{1}{\eta_0}} = \frac{1 - i^h_{gb}}{1 - \frac{i^h_{gb}}{\eta_0}} \tag{21}$$

Similarly, for a transmission in which the carrier h remains the driving member but a different stationary element is assigned, the corresponding efficiency expression retains the same general structure, with the indices of the reverted-mechanism ratio exchanged as required by the selected kinematic arrangement. In general form, the efficiency of the k–h–v scheme in reduction mode follows the same mathematical structure as Equation (16), whereas the reverted-mechanism transmission ratio differs from that in the 2k–h scheme by the absence of the negative sign:

$$i^h_{stop-out} = \frac{1}{i^h_{out-stop}} = \frac{Z_{out}}{Z_{stop}} \tag{22}$$

When the carrier becomes the driven member, the mechanism operates in multiplication mode. Applying the same derivation procedure while preserving the functional roles of the corresponding members in the reverted mechanism gives the following:

$$\begin{gathered} i^b_{gh} = 1 - i^h_{gb} \\ i^g_{bh} = 1 - i^h_{bg} \end{gathered} \tag{23}$$

and, for the complementary assignment,

$$\begin{gathered} \frac{T_b}{T_g} = -i^h_{gb} \cdot \eta_0 \\ \frac{T_g}{T_b} = -i^h_{bg} \cdot \eta_0 \end{gathered} \tag{24}$$

Thus, when the satellite acts as the driving member in the k–h–v transmission, the efficiency is obtained as follows:

$$\eta^b_{g-h} = \frac{\left(1 - i^h_{gb}\right) \cdot \eta_0}{1 - i^h_{gb}} \tag{25}$$

In general, therefore, the efficiency of the k–h–v transmission in multiplication mode is described by the same formal structure as Equation (12), with the reverted-mechanism ratio given by the following:

$$i^{h}_{in-stop} = \frac{Z_{stop}}{Z_{in}} \tag{26}$$

The above formulation should be interpreted as an analytical treatment for k–h–v-type planetary transmissions, whose kinematic behavior can be represented by an equivalent reverted-mechanism ratio and whose mesh-related losses can be summarized by an effective reverted-mechanism efficiency. Therefore, the model is not restricted to a single structural realization of the k–h–v family. It is applicable to configurations in which the dominant power-transfer path follows the same reverted-mechanism relation and where additional output-transfer losses are either negligible at the screening stage or treated separately. However, specific k–h–v implementations may include crank, pin, Hooke's-joint, or other output-transfer arrangements. Losses associated with these mechanisms are not included in the closed-form gear-mesh efficiency expression and should be added separately when the net efficiency of a complete transmission is required.

To illustrate the practical behavior of this broader k–h–v formulation, a cycloidal-pin transmission is considered here as a representative high-ratio example rather than as the only applicable configuration. For example, when the difference between the number of pins on the central gear and the number of teeth on the satellite is equal to one, and the parameters satisfy (Z_b = 16) and (Z_g = 15), the reduction-mode efficiency is approximately 0.95, whereas the multiplication-mode efficiency decreases to about 0.81. The absolute value of the transmission ratio in this case is 15. Compared with a 2k–h transmission having the same transmission-ratio magnitude and the same reverted-mechanism efficiency, this representative k–h–v case exhibits lower mesh-related efficiency. In a complete transmission, the net efficiency may be further reduced if losses in the output-transfer mechanism are included.

This comparison indicates that, for the high-ratio example considered here, the k–h–v scheme is less favorable than the 2k–h scheme with a single-rim satellite in terms of mesh-related energy efficiency. At the same time, the k–h–v configuration is subject to an important operational limitation. As shown by the analytical relations, multiplication mode is only feasible when the effective mesh efficiency of the reverted mechanism remains above the loss level required for positive useful output power. Otherwise, the operating point approaches the self-locking boundary, and the multiplier cannot operate effectively.

The dependence of efficiency on reverted-mechanism transmission ratio and meshing losses is summarized in Figure 6. Figure 6a presents the efficiency variation with the reverted-mechanism ratio, whereas Figure 6b shows the corresponding efficiency baseline maps as functions of transmission-ratio magnitude under different reverted-mechanism loss levels.

The trends in Figure 6 show that the reduction mode efficiency decreases gradually with increasing transmission-ratio magnitude, whereas the multiplication mode becomes markedly more sensitive to loss amplification. This difference arises because multiplication mode corresponds to reverse power flow through the k–h–v mechanism. Under this condition, mesh losses are amplified by the transmission-ratio structure, and a progressively larger fraction of the input power is consumed internally as the absolute value of the transmission ratio increases. Consequently, the useful output power decreases rapidly, and the calculated efficiency may approach zero.

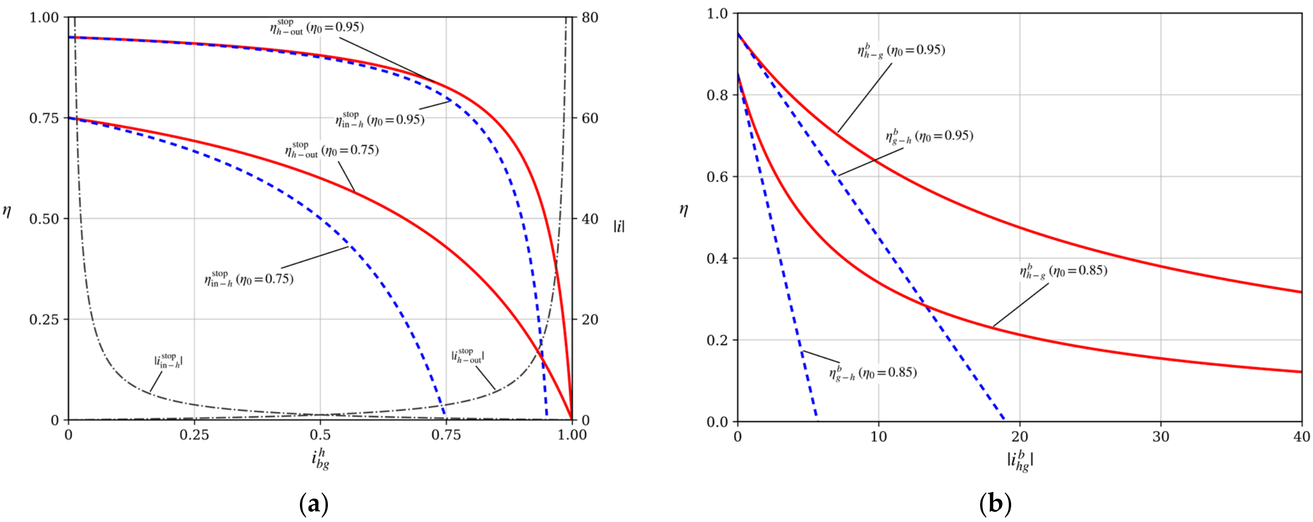

Figure 6. Efficiency characteristics of k–h–v transmissions with single-rim satellites: (**a**) efficiency as a function of reverted-mechanism transmission ratio; (**b**) efficiency baseline maps across transmission-ratio magnitude under different reverted-mechanism loss levels.

This sharp efficiency decrease should be interpreted as the approach to the self-locking boundary defined in Section 2.3 rather than only as a gradual deterioration in transmission quality. When the reverted-mechanism efficiency approaches the corresponding ratio threshold, the available driving power is no longer sufficient to overcome internal losses and maintain positive useful output power in the intended multiplication direction. The multiplier regime of the k–h–v configuration is therefore intrinsically less robust to meshing losses than the corresponding reduction regime. Configurations located close to the low-efficiency region in Figure 6b should be regarded as self-locking-prone and should not be selected for reversible or speed-increasing actuator applications without further verification.

From an engineering-design perspective, these efficiency maps identify operating regions with different levels of robustness to mesh-efficiency deterioration. The gradual efficiency variation in reduction mode provides a comparatively stable design region, whereas the steep deterioration and self-locking tendency in multiplication mode indicate a narrow allowable efficiency margin. Therefore, low-efficiency and self-locking-adjacent regions of the k–h–v scheme should be treated as critical design zones when high-ratio multiplication or reversible operation is required.

3.3. *Efficiency Characteristics of 2k–h Planetary Gear Trains with Double-Rim Satellites*

The use of double-rim satellites in the 2k–h configuration substantially extends the attainable transmission-ratio range relative to the corresponding single-rim arrangement. For the carrier-driven case, the transmission ratio is expressed as follows:

$$i_{ha}^{b} = \frac{\omega_h}{\omega_a} = \frac{i_{ba}^{h}}{i_{ba}^{h} - 1} = \frac{1}{1 - i_{ab}^{h}} \tag{27}$$

At the same time,

$$i_{ba}^{h} = \frac{1}{i_{ab}^{h}} = \frac{Z_a \cdot Z_{g1}}{Z_b \cdot Z_{g2}} \tag{28}$$

For pin-cycloidal transmissions, $Z_{g1} = Z_b - 1$ and $Z_{g2} = Z_a - 1$. Thus,

$$i_{ha}^{b} = \frac{Z_a \cdot (Z_b - 1)}{Z_b - Z_a} \tag{29}$$

The efficiency (η) for the carrier-driven configuration is evaluated using Equation (16), but an adjustment is required. In the 2k–h transmission with a single-rim satellite and in the k–h–v transmission with a single-rim satellite, the central gear a retained the role of the driven link in the reverted mechanism. In the double-rim-satellite configuration, however, different tooth-number combinations may lead to different functional roles of element a during the reverted motion. When the carrier is the driving link, the transmission efficiency, following Equation (14), is written as follows:

$$\eta_{ha}^{b} = -\frac{P_a}{P_h} = -\frac{T_a \cdot \omega_a}{(T_a + T_b) \cdot \omega_h} = \frac{1}{\left(1 + \frac{T_b}{T_a}\right) \cdot i_{ha}^{b}} \quad (30)$$

Two possible power-loading cases must be distinguished. In the first case, shown in Figure 7a, the transmission ratio $i_{bha} < 0$. The driving and driven shafts therefore rotate in opposite directions, whereas the torques acting on these shafts have the same direction. In the second case, shown in Figure 7b, the transmission ratio i_{bha} is positive. In this situation, the driving and driven shafts rotate in the same direction, while the corresponding torques act in opposite directions.

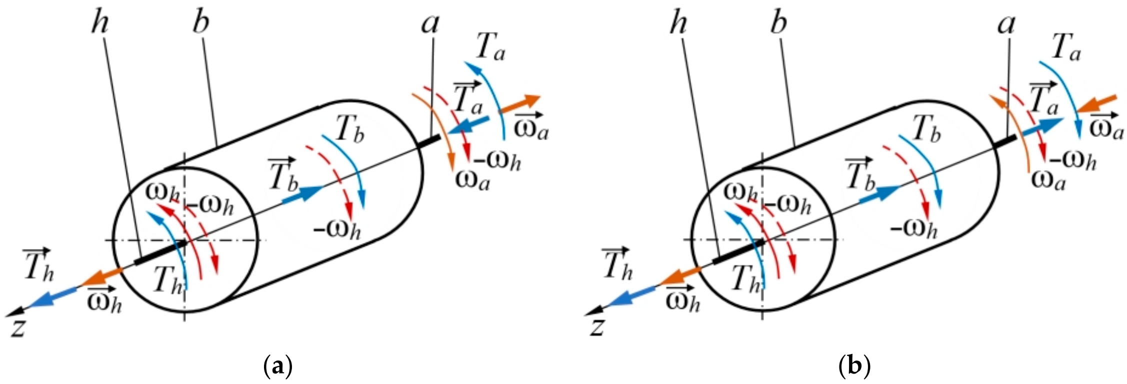

Figure 7. Directions of angular velocities and torques in a 2k–h transmission with a double-rim satellite: (**a**) element a acts as the driven member in the reverted mechanism; (**b**) element a acts as the driving member in the reverted mechanism.

The torque ratio T_b/T_a in Equation (30) is determined from the efficiency equation of the reverted mechanism. In this analysis, the links of the reverted mechanism are assigned an angular velocity equal to $-\omega_h$. In the first case, the angular velocity ω_a retains, and increases in magnitude with, its negative value, which corresponds to the driven-link function, since the directions of torque T_a and angular velocity ω_a are opposite when $T_a > 0$. The corresponding efficiency of the reverted mechanism is then defined as $\eta_0 = P_a/P_b$. In the second case, shown in Figure 7b, if $\omega_a - \omega_h > 0$, element a remains the driven link. If $\omega_a - \omega_h < 0$, the rotation direction changes so that it coincides with the torque direction, and element a becomes the driving link. In that case, the reverted-mechanism efficiency is defined as $\eta_0 = P_b/P_a$.

After transformations analogous to those discussed in the preceding sections, the torque-ratio expressions for the first and second cases are obtained, respectively, as follows:

$$\begin{aligned} \frac{T_b}{T_a} &= -\frac{1}{\eta_0 \cdot i_{ba}^{h}} \\ \frac{T_b}{T_a} &= -\frac{\eta_0}{i_{ba}^{h}} \end{aligned} \quad (31)$$

In the first case, the efficiency can be evaluated using Equation (14) with analogous transformations, and in general form it corresponds to Equation (16). In the second case, the condition $\omega_a - \omega_h < 0$ can be rewritten as $i_{bha} > 1$. The transmission efficiency can then be evaluated using Equation (12), with the numerator and denominator exchanged and the indices of the input and output members adjusted accordingly.

Thus, the generalized form corresponding to Equation (16) becomes the following:

$$\eta^{stop}_{h-out} = \frac{1 - i^{h}_{out-stop}}{i^{h}_{out-stop}} \cdot \frac{1}{1 - \frac{1}{\eta_0}^{sign(1 - i^{-stop}_{h-out})}} = \frac{i^{h}_{stop-out} - 1}{i^{h}_{stop-out}} \cdot \frac{1}{\frac{1}{\eta_0}^{sign(1 - i^{-stop}_{h-out})}} \tag{32}$$

The second case corresponds to a multiplier mechanism with a double-rim satellite and a driving carrier, which cannot be realized in 2k–h transmissions with a single-rim satellite. If required, the efficiency can also be expressed solely through the transmission ratios of generalized mechanisms. This is achieved by substituting the ratio $i_{stop-out}$ in Equation (32) using the corresponding kinematic relations, where the generalized ratios are adapted to the specific 2k–h or k–h–v configuration. In the following form:

$$i^{stop}_{h-out} = \frac{1}{1 - i^{h}_{out-stop}} = \frac{i^{h}_{stop-out}}{i^{h}_{stop-out} - 1} \tag{33}$$

To analyze Equation (32), the transmission efficiency for the carrier-driven case may be represented as a function of reverted-mechanism efficiency and of the gear ratio $i_{stop-out}$ over a wide variation range. The resulting efficiency graph consists of two branches that decrease as the absolute value of the abscissa increases, with a maximum at $i_{stop-out} = 1$. At this point, the efficiency becomes unity, indicating that neither reduction nor multiplication occurs and that the driving and driven shafts rotate together without relative motion. For clarity and easier comparison, the left branch of the graph $\left(i_{stop-out} < 1\right)$ is reflected to the right side of the point $i_{stop-out} = 1$. The ordinate values calculated from Equation (33) are therefore plotted against abscissa values corresponding to $-i_{stop-out} + 2$, as shown in Figure 8a.

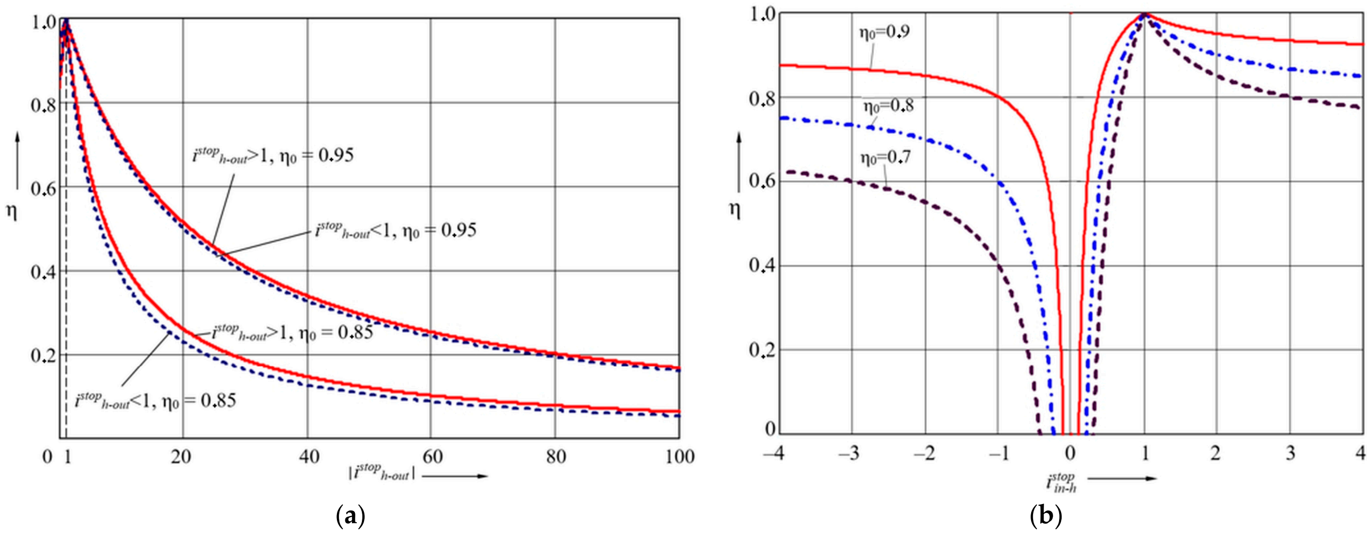

Figure 8. Efficiency baselines of 2k–h planetary gear trains with double-rim satellites: (**a**) carrier-driven configuration; (**b**) driven-carrier configuration.

The two branches in Figure 8 should be interpreted not only as mathematical branches of the efficiency expression, but also as different internal power-flow and torque-balance states. In the co-directional branch, the driving and driven shafts rotate in the same direction. Under this condition, part of the torque effect associated with the input and output members is mutually compensated in the reaction taken by the stationary member. The housing therefore carries a lower resultant reaction torque, and less internal power circulation is associated with the same nominal transmission-ratio magnitude. This explains why the co-directional branch provides a more favorable combination of higher efficiency and lower housing loading.

By contrast, in the opposite-rotation branch, the driving and driven shafts rotate in opposite directions. The corresponding torque reactions tend to add rather than compensate, which increases the reaction torque transmitted to the housing. This branch is therefore associated with a less favorable internal power-flow condition and a higher structural-loading demand on the fixed member. The lower efficiency of this branch is therefore not only a numerical consequence of the analytical expression, but also reflects the less favorable torque-balance condition required to sustain the opposite shaft-rotation directions.

Similarly, Equation (12) can be generalized for 2k–h transmissions with a driving central gear and a driven carrier. When $0 < i_{stop-in-h} < 1$, the driving wheel in the reverted mechanism becomes the driven element, and this role change must be taken into account. The resulting general expression is

$$\eta_{in-h}^{stop} = \frac{1 - \eta_0^{\,sign\left(\frac{i_{in-h}^{stop}-1}{i_{in-h}^{stop}}\right)} \cdot i_{in-stop}^{h}}{1 - i_{in-stop}^{h}} = \frac{i_{stop-in}^{h} - \eta_0^{\,sign\left(\frac{i_{in-h}^{stop}-1}{i_{in-h}^{stop}}\right)}}{i_{stop-in}^{h} - 1} \tag{34}$$

The corresponding efficiency curves are shown in Figure 8b. In this case, the efficiency varies across three intervals of the transmission ratio, namely, $i_{stop-in-h} < 0$, $0 < i_{stop-in-h} < 1$, and $i_{stop-in-h} > 1$. The variation in the third interval has already been discussed in connection with Figure 5.

Thus, the horizontal axis in Figure 8a represents the absolute values of the transmission ratios. In this panel, solid lines correspond to efficiency values when $i_{stop-out} > 1$, whereas dashed lines correspond to $i_{stop-out} < 1$. A comparative analysis indicates that implementing the same transmission-ratio magnitude is more favorable when the driving and driven shafts rotate in the same direction. For pin-cycloidal transmissions, according to Equation (29), this corresponds to the condition $Z_b > Z_a$. Under this condition, the efficiency is higher, and the advantage becomes more pronounced as the efficiency of the reverted mechanism decreases. An additional benefit is a lower moment acting on the housing, because, according to the scheme in Figure 7a, the torque on the stationary wheel compensates for the combined effect of the two co-directional torques T_a and T_h, that is, $T_b = T_h - T_a$. When the driving and driven shafts rotate in opposite directions, the housing torque becomes higher for the same kinematic characteristics, namely, $T_b = T_h + T_a$.

The theoretical possibility of obtaining highly efficient multiplier mechanisms in the transmission-ratio interval from -1 to 1 cannot, however, be realized for some designs. For example, analysis of Equation (29) shows that this interval cannot be achieved for any ratio of Z_a to Z_b.

Figure 8b further shows that, as the absolute value of the transmission ratio increases, the efficiency curves asymptotically approach η_0. The approach occurs from different directions depending on the interval: the efficiency increases toward η_0 when $i_{(in-h)}^{stop} < 0$, but decreases toward η_0 when $i_{(in-h)}^{stop} > 1$. This behavior highlights the broader and more differentiated efficiency landscape of the double-rim 2k–h configuration relative to the single-rim arrangement.

From a mechanical-design perspective, the double-rim 2k–h configuration is especially informative because the two efficiency branches correspond to different torque-reaction characteristics. For the same nominal transmission-ratio magnitude, the branch with co-directional shaft rotation provides a more favorable combination of higher efficiency and lower housing torque. The opposite-rotation branch is less favorable because it increases the torque reaction on the housing and may impose higher demands on support stiffness, bearing selection, and structural design. This branch-dependent behavior should therefore be considered together with transmission ratio and mesh efficiency during layout screening.

4. Discussion

The analytical results show that the efficiency behavior of planetary gear trains is governed by the combined effects of mesh-loss level, kinematic layout, operating mode, and functional assignment of the driving, driven, and stationary members. This finding is consistent with recent power-flow-oriented modelling studies showing that efficiency and power ratio in compound planetary gear trains depend on how subsystem connections, constraints, and power-flow paths are represented [31]. In the present formulation, keeping the member functions explicit makes it possible to compare reduction and multiplication modes within the same sign convention and reverted-mechanism framework. For the 2k–h transmission with a single-rim satellite, reduction and multiplication modes show nearly overlapping efficiency-ratio trends when the reverted-mechanism efficiency is high. As the reverted-mechanism efficiency decreases, however, multiplication mode becomes more sensitive to loss amplification. This indicates that the same nominal transmission-ratio magnitude may lead to different efficiency penalties depending on whether the gear train operates as a reducer or as a multiplier.

The k–h–v configuration presents a more restrictive efficiency response, particularly in multiplication mode and near the self-locking boundary. In these regions, a small reduction in reverted-mechanism efficiency can produce a disproportionately large decrease in the calculated transmission efficiency. This result is mechanically important because it identifies operating regions where apparently moderate mesh losses may strongly affect power demand, heat generation, and transmission feasibility. The rapid efficiency decrease in multiplication mode should therefore be interpreted not only as low efficiency, but also as a warning that the mechanism is approaching a self-locking-prone region. Recent modelling work on planetary gear trains has also shown that structural flexibility, multi-tooth meshing, and ring/carrier deformation can significantly influence tooth loads and vibration behavior [32]. Although these effects are outside the compact analytical scope of the present study, they reinforce the need to retain sufficient efficiency margin when selecting high-ratio planetary layouts, especially for configurations close to self-locking or multiplier-sensitive regions.

The double-rim 2k–h configuration further demonstrates that branch-dependent behavior is an essential design consideration. For the same nominal transmission-ratio magnitude, the branch with co-directional rotation of the driving and driven shafts gives higher efficiency and lower housing torque. This behavior can be explained by the internal power-flow direction and torque balance. In the co-directional branch, part of the torque effect associated with the input and output members is mutually compensated in the reaction taken by the stationary member. The housing therefore carries a lower resultant reaction torque, and less internal power circulation is associated with the same nominal transmission-ratio magnitude. By contrast, in the opposite-rotation branch, the torque reactions tend to add rather than compensate. This increases the reaction torque transmitted to the housing and produces a less favorable internal power-flow condition. The branch-dependent efficiency difference is therefore not only a numerical result of the analytical expression, but also reflects the different structural-loading conditions required to sustain the corresponding shaft-rotation directions.

This distinction is mechanically relevant because housing torque affects support loading, shaft and bearing reactions, and the distribution of structural forces in practical gear units. Recent planetary-gear dynamic studies have shown that mesh phasing, position errors, and vibration modulation can strongly influence planetary-gear response [33]. Therefore, the branch-dependent torque behavior observed here should not be interpreted only as an efficiency result, but also as a design signal for subsequent structural, dynamic, and load-sharing evaluation. For actuator-oriented applications, this is particularly important because a transmission branch that appears acceptable from the transmission-ratio requirement alone may impose higher housing reaction, bearing loading, or structural demand than an alternative branch with the same nominal ratio.

The engineering significance of these efficiency differences can be illustrated by the duty-cycle calculation considered in this study. Increasing gear-train efficiency from 0.85 to 0.92 reduces the required motion energy by approximately 7–8% for the same mechanical task. Although this estimate is simplified, it demonstrates that moderate efficiency improvements at the transmission level can translate into measurable energy savings under repeated operation. For actuator-driven systems, such savings may influence motor sizing, thermal loading, battery demand, operating temperature, and permissible duty cycle [34]. The analytical results therefore provide more than a purely kinematic comparison; they indicate how layout selection and mode selection can affect system-level energy use.

It is important, however, to distinguish the mesh-related efficiency baseline obtained in this study from the total efficiency of a complete gearbox. The reverted-mechanism efficiency used in the analytical expressions represents the effective loss level associated with gear meshing in the corresponding reverted mechanism. Detailed power-loss prediction in real gear units usually requires more specific information about surface roughness, lubrication regime, contact conditions, speed, load, and temperature. Recent gear power-loss models based on stochastic microcontact descriptions and tribological analysis have shown that mechanical power loss is strongly affected by local contact and lubrication conditions [35]. Similarly, tribo-dynamic modelling of planetary gear bearing systems has shown that helical gear meshing, bearing deformation, friction, lubrication, contact, and wear can be strongly coupled in practical planetary systems [36]. These studies highlight why the present analytical model should be viewed as a baseline for early screening rather than as a replacement for detailed tribological modelling.

Non-mesh losses require particular attention when the analytical baseline is transferred to a fully specified actuator gearbox. Bearing losses, seal losses, windage, lubricant agitation, and oil-churning losses are not explicitly included in the closed-form efficiency expressions derived in this study. These losses may be relatively small in low-speed or lightly lubricated preliminary comparisons, but they can become significant in high-speed planetary reducers, oil-bath transmissions, compact sealed actuator gearboxes, or heavily loaded bearing arrangements. In such cases, the total gearbox efficiency should be evaluated by correcting the present mesh-related baseline with additional bearing, seal, windage, churning, thermal, and design-specific loss terms. The present formulation therefore provides the mesh-efficiency component of the efficiency assessment, while full gearbox evaluation requires supplementary loss modelling or experimental calibration.

The present framework intentionally remains compact by representing local mesh losses through the reverted-mechanism efficiency. This simplification is appropriate when the objective is to compare layouts, operating modes, self-locking tendencies, and housing-torque behavior before detailed geometry, lubrication, bearing arrangement, and housing design are fixed. In later design stages, the analytical baselines can be coupled with more detailed models of mesh stiffness, profile modification, sliding loss, thermal response, and dynamic excitation. Recent work has shown that profile modification affects static and dynamic transmission error and is commonly used to improve geared-system behavior under design and off-design conditions [37]. More recent optimization studies have further integrated macro- and micro-geometry design to reduce gear mesh power loss and transmission error simultaneously [38], while integrated profile-modification and partial-EHL approaches have been used to evaluate sliding power losses in spur gears [39]. These developments indicate a practical route for extending the present framework: the closed-form efficiency baselines can first identify promising planetary layouts and sensitive operating regions, after which high-fidelity tooth-contact, lubrication, and dynamic models can be applied only to the most relevant configurations [40].

Compared with detailed tribological, elastohydrodynamic, CFD-based churning, thermal-network, or multibody-dynamic models, the present formulation requires only direct evaluation of closed-form expressions once the topology, transmission ratio, functional member assignment, and reverted-mechanism efficiency are specified. Its computational burden is therefore negligible for each candidate configuration and does not require iterative tooth-contact solving, coupled thermal–lubrication simulation, or time-domain dynamic analysis. This makes the framework suitable for rapid screening of many actuator-transmission schemes during preliminary design. The main value of the approach is not to replace high-fidelity gearbox modelling, but to reduce the design space before such models are applied. In this sense, the analytical framework provides a lightweight and transparent decision-support tool for early-stage actuator-transmission selection.

5. Conclusions

This study developed a unified analytical framework for estimating the transmission efficiency of involute planetary gear trains used in actuator-oriented mechanical systems. Based on power balance, Willis' relation, and torque equilibrium along the transmission axis, compact closed-form efficiency expressions were derived for common 2k–h and k–h–v layouts, covering single- and double-rim satellites, reduction and multiplication modes, and different assignments of driving, driven, and stationary members. By representing mesh losses through the efficiency of the reverted mechanism, the formulation provides a consistent basis for comparing efficiency behavior across planetary-gear configurations within the same sign convention and power-flow interpretation. The results show that reduction and multiplication modes exhibit nearly identical efficiency-ratio trends when the reverted-mechanism efficiency is high, whereas multiplication mode becomes more sensitive to loss amplification as mesh efficiency decreases; this effect is especially important for k–h–v configurations, where the multiplication-mode efficiency may decrease sharply and approach the self-locking boundary. For the 2k–h transmission with a double-rim satellite, branch-dependent behavior is observed, with the co-directional rotation branch providing higher efficiency and lower housing-reaction torque than the opposite-rotation branch. The duty-cycle calculation further indicates that increasing gear-train efficiency from 0.85 to 0.92 reduces the required motion energy by approximately 7–8% for the same mechanical task. Although bearing losses, seal losses, lubricant churning, windage, thermal transients, tooth-contact deformation, structural flexibility, and vibration effects are not explicitly resolved in the closed-form expressions, the proposed framework provides a mesh-related analytical baseline that can be corrected by additional loss terms, detailed tribological and dynamic models, or experimental calibration during later design stages. Overall, the framework offers a lightweight and computationally efficient basis for early-stage planetary-transmission screening, helping to identify configurations with favorable efficiency, lower housing-reaction torque, reduced susceptibility to self-locking, and better actuator-transmission suitability before detailed tooth-contact modelling, thermal analysis, dynamic simulation, or prototype testing is undertaken.

Author Contributions: Conceptualization, H.P., M.E.L., and Y.N.; methodology, H.P. and M.E.L.; formal analysis, H.P., M.E.L., and A.K.; investigation, H.P., A.K., and G.L.; validation, M.E.L., A.K., and G.L.; resources, M.E.L. and G.L.; data curation, H.P. and Y.N.; writing—original draft preparation, H.P. and Y.N.; writing—review and editing, M.E.L., A.K., G.L., and Y.N.; visualization, H.P. and Y.N.; supervision, M.E.L.; project administration, M.E.L. and Y.N. All authors have read and agreed to the published version of the manuscript.

Funding: This research received no external funding.

Institutional Review Board Statement: Not applicable.

Informed Consent Statement: Not applicable.

Data Availability Statement: All data generated or analyzed during this study are included in this published article.

Conflicts of Interest: The authors declare no conflicts of interest.

Abbreviation

The following abbreviation is used in this manuscript:

PGT	Planetary gear train

References

1. Arnaudov, K.; Karaivanov, D.P. *Planetary Gear Trains*; CRC Press: Boca Raton, FL, USA, 2019.
2. García, P.L.; Crispel, S.; Saerens, E.; Verstraten, T.; Lefeber, D. Compact Gearboxes for Modern Robotics: A Review. *Front. Robot. AI* **2020**, *7*, 103. [CrossRef] [PubMed]
3. Zhou, M.; Xu, T.; Wang, G.; Dong, H.; Yang, S.; Wang, Z. Design of a 2R Open-Chain Plug Seedling-Picking Mechanism and Control System Constrained by a Differential Non-Circular Planetary Gear Train. *Agriculture* **2024**, *14*, 1576. [CrossRef]
4. Tang, Z.; Zhang, H.; Li, H.; Li, Y.; Ding, Z.; Chen, J. Developments of Crawler Steering Gearbox for Combine Harvester Straight Forward and Steering in Situ. *Int. J. Agric. Biol. Eng.* **2020**, *13*, 120–126. [CrossRef]
5. Zhou, M.; Yang, J.; Xu, T.; Ying, J.; Wang, X. Optimal Design of Transplanting Mechanism with Differential Internal Engagement Non-Circular Gear Trains. *J. Agric. Eng.* **2022**, *53*, 1412. [CrossRef]
6. Habermehl, C.; Jacobs, G.; Neumann, S. A Modeling Method for Gear Transmission Efficiency in Transient Operating Conditions. *Mech. Mach. Theory* **2020**, *153*, 103996. [CrossRef]
7. Li, L.; Shao, Z.; Liu, W.; Liu, Y.; Zhao, S.; Wei, Y.; Zhang, J.; Wang, X.; Hou, H. Channel Microenvironment-Controlled Pillared MOF as Efficient Triboelectric Nanogenerator Material for Self-Powered Degradation of Organic Pollutants. *Energy Environ. Mater.* **2026**, e70280. [CrossRef]
8. Zhou, M.; Yang, Y.; Wei, M.; Yin, D. Method for Generating Non-Circular Gear with Addendum Modification and Its Application in Transplanting Mechanism. *Int. J. Agric. Biol. Eng.* **2020**, *13*, 68–75. [CrossRef]
9. Zhou, M.; Yang, J.; Yin, J.; Wang, Z. Design Method and Experimental Study of a Rice Transplanting Mechanism with Three Planting Arms Constrained by Differential Noncircular Gear Trains. *J. ASABE* **2022**, *65*, 221–233. [CrossRef]
10. Zhou, M.; Wang, G.; Xu, T.; He, J.; Deng, Y.; Li, X. Trajectory Matrix-Guided Optimal Design of Non-Circular Gear Train Seedling Throwing Mechanism for Rice Pot Seedlings. *Sci. Rep.* **2026**, *16*, 13180. [CrossRef] [PubMed]
11. Aroua, A.; Defreyne, P.; Verbelen, F.; Lhomme, W.; Bouscayrol, A.; Sergeant, P.; Stockman, K. Power Loss Scaling Laws of High-Speed Planetary Reducers. *Mech. Mach. Theory* **2023**, *189*, 105428. [CrossRef]
12. Concli, F.; Conrado, E.; Gorla, C. Analysis of Power Losses in an Industrial Planetary Speed Reducer: Measurements and Computational Fluid Dynamics Calculations. *Proc. Inst. Mech. Eng. Part J J. Eng. Tribol.* **2014**, *228*, 11–21. [CrossRef]
13. Liang, Z.; Li, Y.; Xu, L.; Zhao, Z.; Tang, Z. Optimum Design of an Array Structure for the Grain Loss Sensor to Upgrade Its Resolution for Harvesting Rice in a Combine Harvester. *Biosyst. Eng.* **2017**, *157*, 24–34. [CrossRef]
14. Yao, M.; Hu, J.; Liu, W.; Shi, J.; Jin, Y.; Lv, J.; Sun, Z.; Wang, C. Precise Servo-Control System of a Dual-Axis Positioning Tray Conveying Device for Automatic Transplanting Machine. *Agriculture* **2024**, *14*, 1431. [CrossRef]
15. Liang, Z.; Li, J.; Liang, J.; Shao, Y.; Zhou, T.; Si, Z.; Li, Y. Investigation into Experimental and DEM Simulation of Guide Blade Optimum Arrangement in Multi-Rotor Combine Harvesters. *Agriculture* **2022**, *12*, 435. [CrossRef]
16. del Castillo, J.M. The Analytical Expression of the Efficiency of Planetary Gear Trains. *Mech. Mach. Theory* **2002**, *37*, 197–214. [CrossRef]

17. Mantriota, G.; Pennestrì, E. Theoretical and Experimental Efficiency Analysis of Multi-Degrees-of-Freedom Epicyclic Gear Trains. *Multibody Syst. Dyn.* **2003**, *9*, 389–408. [CrossRef]
18. Pennestrì, E.; Freudenstein, F. The Mechanical Efficiency of Epicyclic Gear Trains. *J. Mech. Des.* **1993**, *115*, 645–651. [CrossRef]
19. Yang, F.; Feng, J.; Zhang, H. Power Flow and Efficiency Analysis of Multi-Flow Planetary Gear Trains. *Mech. Mach. Theory* **2015**, *92*, 86–99. [CrossRef]
20. Chen, H.; Chen, X.-A. Recirculation of Parallel-Connected Planetary Gear Trains. *Chin. J. Mech. Eng.* **2022**, *35*, 27. [CrossRef]
21. Yin, J.; Chen, Z.; Lv, S.; Wu, H.; Gao, Y.; Wu, L. Design and Fatigue Life Analysis of the Rope-Clamping Drive Mechanism in a Knotter. *Agriculture* **2024**, *14*, 1254. [CrossRef]
22. Zhang, B.; Bai, T.; Wu, G.; Wang, H.; Zhu, Q.; Zhang, G.; Meng, Z.; Wen, C. Fatigue Analysis of Shovel Body Based on Tractor Subsoiling Operation Measured Data. *Agriculture* **2024**, *14*, 1604. [CrossRef]
23. Yin, J.; Gao, Y.; Guo, R.; Lv, S.; Zhou, M.; Yu, D. Wear Calculation Method of Tripping Mechanism of Knotter Based on Rigid-Flexible Coupling Dynamic Model. *Agriculture* **2025**, *15*, 2229. [CrossRef]
24. Pennestrì, E.; Valentini, P.P. A Review of Formulas for the Mechanical Efficiency Analysis of Two Degrees-of-Freedom Epicyclic Gear Trains. *J. Mech. Des.* **2003**, *125*, 602–608. [CrossRef]
25. Esmail, E.L.; Pennestrì, E.; Hussein Juber, A. Power Losses in Two-Degrees-of-Freedom Planetary Gear Trains: A Critical Analysis of Radzimovsky's Formulas. *Mech. Mach. Theory* **2018**, *128*, 191–204. [CrossRef]
26. Esmail, E.L.; Pennestrì, E.; Cirelli, M. Power-Flow and Mechanical Efficiency Computation in Two-Degrees-of-Freedom Planetary Gear Units: New Compact Formulas. *Appl. Sci.* **2021**, *11*, 5991. [CrossRef]
27. Salgado, D.R.; del Castillo, J.M. Analysis of the Transmission Ratio and Efficiency Ranges of the Four-, Five-, and Six-Link Planetary Gear Trains. *Mech. Mach. Theory* **2014**, *73*, 218–243. [CrossRef]
28. Vasić, M.; Blagojević, M.; Banić, M.; Maccioni, L.; Concli, F. Theoretical and Experimental Investigation of the Thermal Stability of a Cycloid Speed Reducer. *Lubricants* **2025**, *13*, 70. [CrossRef]
29. Zhao, Y.; Han, Z.; Tan, Q.; Shan, W.; Li, R.; Wang, H.; Du, Y. Multi-Objective Optimization Design of Cycloid-Pin Gears Based on RV Reducer Precision Transmission Performance. *Energies* **2024**, *17*, 654. [CrossRef]
30. Lu, Y.; Xu, L. Transmission Efficiency of One Tooth Difference Sine Tooth Profile Planetary Reducer. *Heliyon* **2024**, *10*, e26300. [CrossRef] [PubMed]
31. Geitner, G.-H.; Komurgoz, G. Key Characteristics of Generic Bond Graphs for Planetary Gears. *Mech. Mach. Theory* **2022**, *178*, 105082. [CrossRef]
32. Jianjun, T.; Hao, L.; Hao, T.; Caichao, Z.; Chaosheng, S.; Yehong, D.; Zhangdong, S. Dynamic Modeling and Analysis of Planetary Gear Train System Considering Structural Flexibility and Dynamic Multi-Teeth Mesh Process. *Mech. Mach. Theory* **2023**, *186*, 105348. [CrossRef]
33. Dai, H.; Wang, Y.; Luo, S.; Li, Y.; Zi, B. Dynamic Modeling and Vibration Analysis of Planetary Gear Sets Concerning Mesh Phasing Modulation. *Mech. Syst. Signal Process.* **2023**, *200*, 110557. [CrossRef]
34. Xu, K.; Liu, J.; Huang, H.; Wang, C.; Zhao, W.; Ge, S.S. Multi-Agent Dynamic Surface Consensus Control of Dual-Motor Steer-by-Wire System under Communication Faults. *IEEE Trans. Ind. Electron.* **2026**, 1–12. [CrossRef]
35. Hong, I.; Aneshansley, E.; Chaudhury, K.; Talbot, D. Stochastic Microcontact Model for the Prediction of Gear Mechanical Power Loss. *Tribol. Int.* **2023**, *183*, 108413. [CrossRef]
36. Yin, J.; Meng, X.; Cheng, S.; Fang, X.; Fan, X. Tribo-Dynamics Modeling and Analysis of Planetary Gear Bearing Systems in Wind Turbines Considering Sun-Planetary-Ring Helical Gear Mesh and Elastic Deformation Effects. *Tribol. Int.* **2024**, *200*, 110059. [CrossRef]
37. Autiero, M.; Paoli, G.; Cirelli, M.; Valentini, P.P. The Effect of Different Profile Modifications on the Static and Dynamic Transmission Error of Spur Gears. *Mech. Mach. Theory* **2024**, *201*, 105752. [CrossRef]
38. Kim, S.; Moon, S.; Choi, C.; Sohn, J. Optimal Design Strategy for Gear Pairs Integrating Macro and Micro Geometry Optimization. *Mech. Mach. Theory* **2025**, *214*, 106119. [CrossRef]
39. Autiero, M.; Paoli, G.; Cirelli, M.; Valentini, P.P. Influence of Profile Modifications on Spur Gear Sliding Power Losses: An Integrated Approach with Advanced Mesh Stiffness and Partial EHL. *Mech. Mach. Theory* **2025**, *214*, 106118. [CrossRef]
40. Chen, D.; Xu, C.; Yu, J.; Wang, Q.; Fang, H.; Yin, S.; Lookman, T.; Chen, R. Interpretable Machine Learning Framework for Nb–si Based Alloy Design with Enhanced Fracture Toughness. *Adv. Sci.* **2026**, e75815. [CrossRef] [PubMed]